Interruption of torus doubling bifurcation and genesis of strange nonchaotic attractors in a quasiperiodically forced map: Mechanisms and their characterizations

A. Venkatesan and M. Lakshmanan
Centre for Nonlinear Dynamics, Department of Physics, Bharathidasan University, Tiruchirapalli 620 024, India
(Received 18 May 2000; published 26 January 2001)

A simple quasiperiodically forced one-dimensional cubic map is shown to exhibit very many types of routes to chaos via strange nonchaotic attractors (SNAs) in a two-parameter (A-f) space. The routes include transitions to chaos via SNAs from both a one-frequency torus and a period-doubled torus. In the former case, we identify the fractalization and type-I intermittency routes. In the latter case, we point out that at least four distinct routes for the truncation of the torus-doubling bifurcation and the creation of SNAs occur in this model. In particular, the formation of SNAs through Heagy-Hammel, fractalization, and type-III intermittent mechanisms is described. In addition, it has been found that in this system there are some regions in the parameter space where a dynamics involving a sudden expansion of the attractor, which tames the growth of period-doubling bifurcation, takes place, creating the SNA. The SNAs created through different mechanisms are characterized by the behavior of the Lyapunov exponents and their variance, by the estimation of the phase sensitivity exponent, and through the distribution of finite-time Lyapunov exponents.

DOI: 10.1103/PhysRevE.63.026219 PACS number(s): 05.45.−a

I. INTRODUCTION

Torus-doubling bifurcation (geometrically similar to period-doubling bifurcation) as a universal route to chaos has been one of the leading topics of research in the study of quasiperiodically forced chaotic dynamical systems during the past few years [1–6]. The existence of such an exotic bifurcation in several experimental situations and theoretical models indicates the importance of this bifurcation in improving our understanding of the qualitative and quantitative behaviors of dynamical systems [1–11]. A very common observation is that such systems do not undergo an infinite sequence of doubling bifurcations as in the case of lower dimensional systems; instead, the truncation of torus doubling begins when the doubled torus becomes extremely wrinkled and then gets destroyed. Such a destroyed torus is a geometrically strange (fractal dimensional) object in the phase space, a property that usually corresponds to a chaotic attractor. However, it does not exhibit sensitivity to initial conditions asymptotically (for example, Lyapunov exponents are nonpositive) and hence is not chaotic and so it is a strange nonchaotic attractor (SNA) [12–29]. Actually the existence of SNAs was first identified by Grebogi *et al.* [12] in their work on the transition from a two-frequency torus to chaos via a SNA. Later on, it was found that these attractors can arise in physically relevant situations such as a quasiperiodically forced pendulum [14,22], quantum particles in quasiperiodic potentials [14], biological oscillators [15], Duffing-type oscillators [16–18], velocity-dependent potential systems [11], electronic circuits [19,20], and in certain maps [21–26], with different transitions to SNAs including the torus-doubling bifurcation and the creation of SNAs. Also, the existence of torus-doubling truncation and the appearance of SNAs was confirmed by an experiment on a quasiperiodically forced, buckled magnetoelastic ribbon [27]. Besides this experiment, exotic strange nonchaotic attractors were studied in analog simulations of a multistable potential [28], and in a neon glow discharge experiment [29] through different transitions to SNAs. The existence of SNAs in such physically relevant systems has naturally motivated further intense investigations on their nature and occurrence.

A subject of intense further interest is the way in which the truncation of period doubling creates SNAs. In particular, it has been found that the creation of SNAs often occurs due to the collision of a period-doubled torus with its unstable parent so that a period-2^k torus gives rise to a 2^{k-1}-band SNA [8], or a gradual fractalization of the torus, in which a period-2^k torus approaches a 2^k-band SNA [9]. Recently, the present authors have shown that the torus-doubling sequence is tamed due to a subharmonic bifurcation (subcritical period-doubling bifurcation) leading to the creation of SNAs. In addition, this transition has been shown to exhibit type-III intermittent characteristic scaling [17,19]. Apart from the creation of SNAs due to the collapse of the tori, the authors have also shown that there are some regions of the system parameters where the torus-doubling sequence is truncated by a merging bifurcation leading to the formation of a torus bubble [11], reminiscent of period bubbles in low dimensional systems. Also, using the renormalization group approach, Kuznetsov, Feudal, and Pikovsky have revealed scaling properties both for the critical attractor and for the parameter plane topography near the terminal point of the torus-doubling bifurcation [10] in connection with this collision scenario.

Besides the creation of SNAs through the truncation of torus-doubling bifurcation, several other mechanisms have also been studied in the literature. The most common is gradual fractalization of a torus where an amplitude or phase instability causes the collapse of the torus [9]. This is in fact one of the least understood mechanisms for the formation of SNAs since there is no apparent bifurcation, unlike the torus collision mechanism identified by Pikovsky amd Feudel where a stable torus and an unstable torus collide at a dense set of points, leading to the creation of SNAs [23]. Prasad,

Mehra, and Ramaswamy [21] have shown that a quasiperiodic analog of a saddle-node bifurcation gives rise to SNAs through an intermittent route with the dynamics exhibiting scaling behavior characteristic of type-I intermittency. Yalcinkaya and Lai have shown that an on-off intermittency can be associated with SNA creation through a blow-out bifurcation when a torus loses its transverse stability [18]. Other than these scenarios, a number of other quasiperiodic routes to SNAs have been described in the literature [13,25]. They include the existence of SNAs in the transition from two-frequency to three-frequency quasiperiodicity [13], transition from three-frequency quasiperiodicity to chaos via a SNA, and transition to chaos via strange nonchaotic trajectories on a torus [25].

Considering particularly the different routes discussed above for the inhibition of the torus-doubling sequence and the creation of SNAs, we note that they have so far been identified essentially in *different* dynamical systems. However, it is important to study the truncation of the torus-doubling bifurcations and the appearance of SNAs in a single system in order to understand the mechanisms and their characteristic features clearly. In this connection, we consider a simple model in the form of a one-dimensional cubic map,

$$x_{i+1} = -Ax_i + x_i^3, \tag{1}$$

which is quite analogous to the typical Duffing oscillator [30,31]. The existence of different dynamical features of this system has been studied in Refs. [31,32]. In the present work, we investigate the dynamics of (1) with the addition of a constant bias,

$$x_{i+1} = Q - Ax_i + x_i^3, \tag{2}$$

and also subject to an additional quasiperiodic forcing,

$$x_{i+1} = Q + f\cos(2\pi\theta_i) - Ax_i + x_i^3,$$

$$\theta_{i+1} = \theta_i + \omega(\mathrm{mod}\ 1), \tag{3}$$

and show that the latter is a rich dynamical system in comparison with the former, possessing a vast number of regular, strange nonchaotic and chaotic attractors in a two-parameter $(A\text{-}f)$ space for a fixed Q. In particular, we focus our attention mainly on the truncation of torus-doubling bifurcations leading to the creation of SNAs and the mechanisms by which they arise in a range of the two-parameter $(A\text{-}f)$ space, besides pointing out the standard transitions to chaos via SNAs from a one-frequency torus. A variety of transitions from a truncated doubled torus to SNAs can be identified, characterized, and distinguished in this system.

To start with, we show that the system (2) undergoes one or more period doublings but it need not complete the entire Feigenbaum cascade, and that it may be possible to have only a finite number of period doublings, followed by, for example, undoubling or other bifurcations in the presence of constant bias, as was shown by Bier and Bountis in different systems [32]. The possibility of such a different remerging bifurcation phenomenon in the torus-doubling sequence is reported in the present case, when the system (2) is subjected to quasiperiodic forcing as in model (3). As the system (3) possesses more than one control parameter and remains invariant under reflection symmetry, remerging is likely to occur, as in the absence of quasiperiodic forcing in the system (2). Our numerical study shows that for a fixed value of Q in some regions of the $(A\text{-}f)$ parameter space a torus-doubled orbit emerges and remerges from a single-torus orbit at two different parameter values of f to form a single torus bubble. Such a remerging bifurcation can retard the growth of the torus-doubled bifurcations and the development of the associated universal route to chaos further. However, the nature of the remerging torus-doubled bifurcation or, more specifically, the torus bubbling ensures the existence of different routes for the creation of SNAs when the full range of parameters is explored. To illustrate such possibilities in the present system in the two-parameter $(A\text{-}f)$ space, we first enumerate three standard types of route to a SNA, namely, (1) the Heagy-Hammel (collision of the period-doubled torus with its unstable parent), (2) the gradual fractalization (amplitude or phase instability), and (3) the type-III intermittency (subharmonic instability) routes through which the truncation of torus-doubling bifurcation occurs, leading to the creation of SNAs within the torus bubble region.

In addition, we identify that in some cross sections of the $(A\text{-}f)$ parameter space, particularly within the torus bubble region, the period-doubling bifurcation phenomenon still persists in the destroyed torus, even though the actual doubling of the torus itself has been terminated. However, we show that *the dynamics involved in this transition is a sudden expansion in the attractor*. This transition looks like the interior crisis that occurs in low dimensional chaotic systems [33]. We also demonstrate the occurrence of SNAs through gradual fractalization and type-I intermittency, during the transition from one-frequency quasiperiodicity to chaos that exists outside the torus bubble region.

In all our studies the transitions to different SNAs at different parts of the border in the $(A\text{-}f)$ parameter plane and their characterization are carried out on the basis of specific quantities such as Lyapunov exponents and their variance as well as finite-time Lyapunov exponents, dimensions, power spectral measures, and phase sensitivity exponents. Brief details of these characterizing quantities are given in the Appendix. In Sec. II we describe the phenomenon of the remerging of the Feigenbaum tree in the absence of quasiperiodic forcing in the map (2). The existence of remerging torus-doubling is pointed out in Sec. III. Various transitions to SNAs through the truncated doubled torus are demonstrated in Sec. IV. In particular, the truncation of the torus-doubling bifurcation and the creation of SNAs through torus collision, fractalization, and type-III intermittent mechanisms are explained. Further, a sudden expansion of the attractor causing the truncation of torus-doubling bifurcation and the genesis of a SNA is also demonstrated. In Sec. V, the transition from a one-frequency torus to a SNA through type-I intermittent as well as fractalization mechanisms is described. In Sec. VI the transitions between different SNAs are discussed. In Sec. VII we address the issue of distinguishing among SNAs formed by different routes

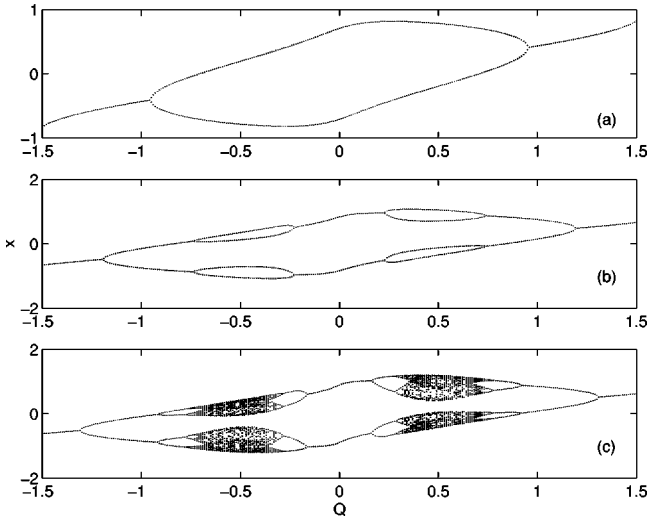

FIG. 1. Bifurcation diagram for the map (2) in the (x,Q) plane. (a) The primary bubble at $A=1.5$, (b) period-2 and period-4 bubbles at $A=1.7$, (c) period-doubling route to chaos and inverse period doubling at $A=1.8$.

through the use of finite-time Lyapunov exponents. Finally, in Sec. VIII, the results are summarized.

II. REMERGING OF FEIGENBAUM TREES IN THE ABSENCE OF QUASIPERIODIC FORCING

To start with, we consider the system (2) and numerically iterate it by varying the values of A and Q. For any Q value and low A values, the system (2) exhibits periodic oscillations with period $1T$. As A increases, a bifurcation occurs and the stable period-T orbit transits into a stable period-$2T$ bubble, as shown in Fig. 1(a). For example, when the value of Q exceeds a certain critical value $Q=-0.99$ for a fixed A, $A=1.5$, a transition from a period-T orbit to a period-$2T$ orbit occurs on increasing Q, essentially due to period-doubling bifurcation. Then the period-$2T$ attractor merges and forms a period-T attractor when the value of Q increases to $Q=0.99$ at the same fixed A. At even higher values of A, $A=1.7$, the primary period-$2T$ bubble bifurcates into secondary period-$4T$ bubbles, as shown in Fig. 1(b). This bubble develops into further bubbles as A gets larger, until an infinitely branched Feigenbaum tree leading to the onset of chaos finally appears, as shown in Fig. 1(c) for $A=1.8$.

Bier and Bountis showed that such a remerging of Feigenbaum trees is quite common in certain models possessing a kind of reflection symmetry property coupled with more than one parameter [32]. Further, they added that the formation of the primary period-$2T$ bubble is seen to lead to higher order bubbles and the development of the associated universal route to chaos in these systems. It is also stated in the literature that the reversal of period doubling occurs when the system possesses a positive Schwarzian derivative at the bifurcation point [34,35]. This is true for the present case that we study. However, there are some counterexamples as pointed out by Nusse and Yorke [35], to show that the positivity of the Schwarzian derivative is not a sufficient condition to rule out period-halving bifurcations.

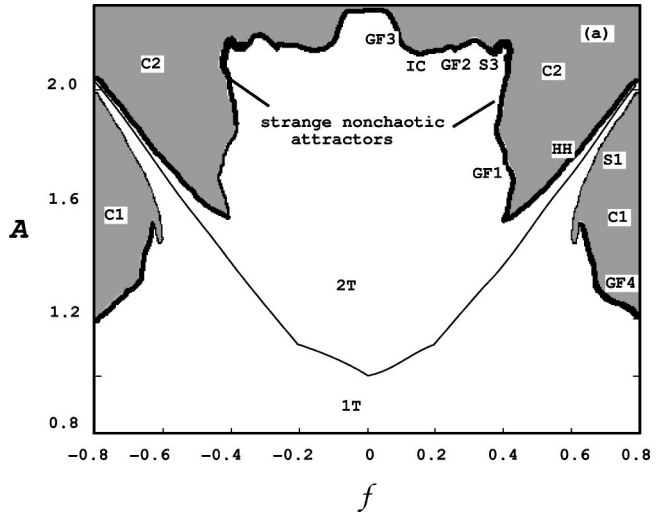

FIG. 2. Phase diagram for quasiperiodically forced cubic map, Eq. (3), in the $(A$-$f)$ parameter space for $Q=0$. Here $1T$ and $2T$ correspond to tori of period 1 and 2, respectively. GF1, GF2, GF3, and GF4 correspond to the regions where the process of gradual fractalization of the torus occurs. HH represents the region where the SNA is created through the Heagy-Hammel route. $S1$ and $S3$ denote regions where the SNA appears through type-I and type-III intermittencies, respectively. IC denotes the region where the SNA is created through crisis-induced intermittency. $C1$ and $C2$ correspond to chaotic attractors.

In the present paper, our aim is to investigate the effect of a quasiperiodic forcing on the system (2) as given by Eq. (3). In particular, we point out that, with the addition of quasiperiodic forcing for a fixed Q, the dynamics is dominated by quasiperiodic attractors and transitions to chaos via strange nonchaotic attractors along different routes in contrast to the type of attractors shown in Fig. 1. For this purpose we also work out a two-parameter $(A$-$f)$ phase diagram (Fig. 2) to identify the changes in the dynamics.

III. SNAs IN THE QUASIPERIODICALLY FORCED CUBIC MAP

Now we consider the dynamics of the quasiperiodically driven map (3) and numerically iterate it with the value of the parameter ω fixed at $\omega=(\sqrt{5}-1)/2$ and by varying the values of A and f for different fixed values of Q. The results are then summarized in a suitable two-parameter $(A$-$f)$ phase diagram for each fixed value of Q. Various dynamical behaviors—quasiperiodic, strange nonchaotic, and chaotic attractors—have been identified by characterizing the attractors by quantities such as Lyapunov exponents and their variance as well as finite-time Lyapunov exponents, dimensions, power spectral measures, and phase sensitivity exponents (for details, see the Appendix).

In the absence of external forcing $(f=0)$, from Fig. 1, we can easily check that for fixed Q and for given A the dynamics corresponds to periodic or chaotic attractors. For instance, for $Q=0$ and for any value of A, the system admits a period-2 solution. Similarly, for $Q=0.25$ and $A=1.8$, it is a period-4 orbit, while for $Q=0.5$ and $A=1.8$, it is a chaotic

orbit. We now include the effect of quasiperiodic forcing ($f \neq 0$) and analyze the dynamics involving torus, period-doubled torus and chaos via SNAs. A very clear picture of the various types of transition becomes available for the case $Q=0$ in the region $f \in (-0.8,0.8)$ and $A \in (0.8,2.4)$, while similar structure arises in a larger region for other values of Q. Consequently, we present in the following results for $Q=0$ only in the form of the phase diagram in Fig. 2. The various features indicated in Fig. 2 are summarized and the dynamical transitions are discussed in the following.

The general features of the phase diagram fall into a very interesting pattern. It can be observed from Fig. 2 that the dynamics is symmetric about $f=0$. Therefore, in the following we present the details for the right of the $f=0$ line only. The features are exactly similar in the left half of the diagram. There are two chaotic regions $C1$ and $C2$. Bordering these chaotic regions, one has the regions where the attractors are strange and nonchaotic. Such SNAs are found to appear in a large number of regions under various mechanisms, some of which are marked GF1, GF2, GF3, and GF4, HH, IC, $S1$, and $S3$. Besides the strange nonchaotic and chaotic attractors in the phase diagram Fig. 2, one can also observe different regions where quasiperiodic attractors can be found. In Fig. 2, such regions are marked as $1T$ and $2T$, corresponding to the quasiperiodic attractors of period 1 and period 2, respectively. Fuller details are given below.

For low A and any f value, the system exhibits quasiperiodic oscillations denoted by $1T$ in Fig. 2. On increasing the value of A further, the fascinating phenomenon of the torus bubble appears within a range of values of f. To be more specific, the parameter A is, for example, fixed at $A=1.1$ and then f is varied. For $f=-0.3$, the attractor is a quasiperiodic one ($1T$). As f is increased to $f=-0.18$, the attractor undergoes torus-doubling bifurcation and the corresponding orbit is denoted as $2T$ in Fig. 2. As f is increased further, one then expects that the doubled attractor continues the doubling sequence as in the case of the generic period-doubling phenomenon. Instead, in the present case, the doubled attractor begins to merge into a single attractor at $f=0.18$, leading to the formation of a torus bubble reminiscent of period bubbles in low dimensional systems, as in the previous section. On refixing the parameter A at higher values, one finds that there are two prominent regions of chaotic oscillations $C1$ and $C2$ as shown in Fig. 2. The chaotic region $C1$ exists outside the torus bubble region. That is, it essentially occurs for larger A values, $A>1.2$ and $f>0.6$. On the other hand, the region $C2$ emerges within the torus bubble region. That is, it appears predominantly for even larger values of A, $A>1.549$ and f lying between -0.8 and 0.8. We have identified two interesting dynamical transitions from one-frequency quasiperiodicity to chaos via SNAs outside the torus bubble region. They are (1) gradual fractalization of the torus leading to creation of a SNA (GF4), and (2) the type-I intermittent route leading to the creation of a SNA ($S1$). There also exist at least four types of transition to chaos via SNAs within the torus bubble where the doubling of the torus is interrupted, namely, (1) Heagy-Hammel (HH), (2) gradual fractalization (GF1, GF2, and GF3), (3) type-III intermittent ($S3$), and (4) doubling of destroyed tori routes, through which the torus-doubling bifurcation is truncated and the creation of a strange nonchaotic attractor takes place. The details for each of the regions are given in the following sections.

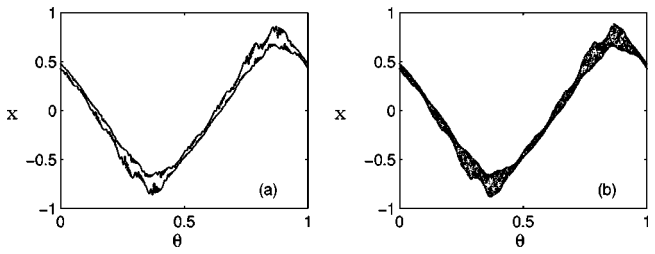

FIG. 3. Projection of the attractors of Eqs. (3) for $f=0.7$ in the (x,θ) plane indicating the transition from quasiperiodic attractor to chaotic attractor via a SNA through the Heagy-Hammel mechanism: (a) wrinkled attractor (period-$2T$) for $A=1.8868$; (b) SNA at $A=1.886\,97$.

IV. DYNAMICS WITHIN THE TORUS BUBBLE

In this section, we will describe each one of the four types of transitions to chaos via SNAs within the torus bubble region in detail.

A. Heagy-Hammel route

The first of the routes that we encounter is the Heagy-Hammel route in which a period-2^n torus gets wrinkled and upon collision with its unstable parent the period-2^{n-1} torus bifurcates into a SNA [8]. Such a route has been identified in the region $C2$ within the range of A values $1.549<A<2.183$ and f values $0.39<f<0.8$. That is, the doubling bifurcation is truncated due to the collision of the doubled torus with its unstable parent on increasing the value of A in the range $1.549<A<2.183$, for a fixed f value ($0.39<f<0.8$). This route is denoted as HH in Fig. 2. For example, let us fix the parameter f at $f=0.7$ and vary A. For $A=1.8$, the attractor is a quasiperiodic one, as denoted by $1T$ in Fig. 2. As A is increased to $A=1.876$, the attractor undergoes torus-doubling bifurcation and the corresponding periodic orbit is denoted as $2T$ in Fig. 2. In the generic case, the period doubling occurs in an infinite sequence until the accumulation point is reached, beyond which chaotic behavior appears. However, with tori, in the present case, the truncation of the torus-doubling begins when the two strands of the $2T$ attractor become extremely wrinkled. For example, when the value of A is increased to $A=1.8868$, the attractor becomes wrinkled as shown in Fig. 3(a). At this transition, the strands are seen to come closer to the unstable period-$1T$ orbit, lose their continuity when the strands of the torus-doubled orbit collide with the unstable parent, and ultimately result in a fractal attractor as shown in Fig. 3(b) when A is increased to $A=1.886\,97$. At such a value, the attractor, Fig. 3(b), possesses a geometrically strange property but does not exhibit any sensitivity to initial conditions [the maximal Lyapunov exponent is negative as seen in Fig. 4(a)] and so it is indeed a strange nonchaotic attractor. At this transition, the two branches of the wrinkled attractor collide and form a one-band SNA. This kind of transition is similar to the at-

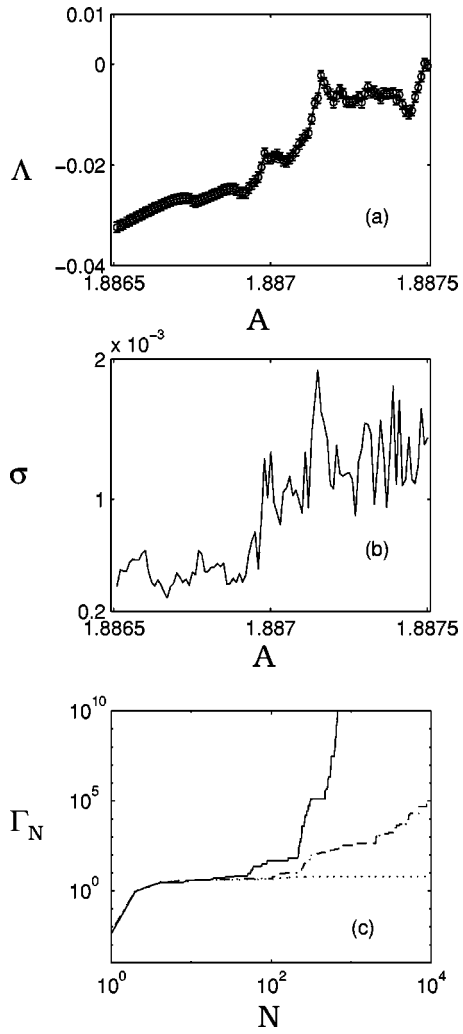

FIG. 4. Transition from doubled torus to SNA through Heagy-Hammel mechanism in the region HH: (a) the behavior of the Lyapunov exponent (Λ); (b) the variance (σ); (c) plot of phase sensitivity function Γ_N vs N (dotted line corresponds to torus for $A=1.83$, dashed line belongs to SNA for $A=1.886\,97$, and solid line represents chaos for $A=1.8878$).

tractor merging crisis occurring in chaotic systems [33]. As A is increased further to $A=1.8878$, the attractor eventually has a positive Lyapunov exponent and hence it corresponds to a chaotic attractor ($C2$).

Now we examine the Lyapunov exponent for the transition from torus to SNA. Figure 4(a) is a plot of the maximal Lyapunov exponent as a function of A for $f=0.7$. When we examine this in a sufficiently small neighborhood of the critical value $A_{HH}=1.886\,97$, the transition is clearly revealed by the Lyapunov exponent, which varies smoothly in the torus region ($A<A_{HH}$) while it varies irregularly in the SNA region ($A>A_{HH}$). It is also possible to identify this transition point by examining the variance of the Lyapunov exponent, as shown in Fig. 4(b), in which the fluctuation is small in the torus region while it is large in the SNA region.

In addition, in order to distinguish the quasiperiodic attractor and the strange nonchaotic attractor, we may examine the attractor with reference to the phase θ of the external

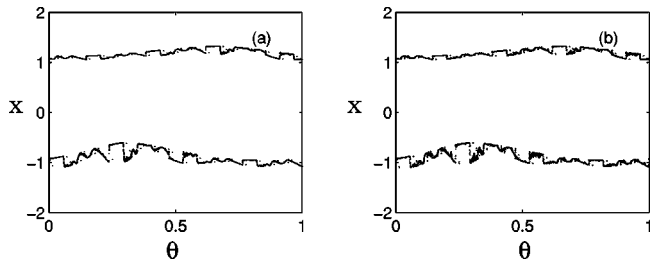

FIG. 5. Projection of the attractors of Eqs. (3) for $f=0.1$ in the (x,θ) plane indicating the transition from quasiperiodic attractor to chaotic attractor via a SNA through the gradual fractalization mechanism: (a) wrinkled attractor (period $2T$) for $A=2.165$; (b) SNA at $A=2.167$.

force. The details of this analysis are given in the Appendix. From Eq. (A4), one infers that the function Γ_N grows infinitely for a SNA with some relation such as $\Gamma_N=N^{\mu}$, where μ is a positive quantity that characterizes the SNA; we may call it the phase sensitivity exponent. For the present case, it is $\mu=0.98$. However, in the case of a chaotic attractor, it grows exponentially with N [see Fig. 4(c)].

B. Fractalization route

The second of the routes is the gradual fractalization route where a torus gets increasingly wrinkled and then transits to a SNA without interaction (unlike the previous case) with a nearby unstable orbit as we change the system parameter. In this route, a period-2^n torus becomes wrinkled and then the wrinkled attractor gradually loses its smoothness and forms a 2^n-band SNA as we change the system parameter. Such a phenomenon has been identified in the present system in three different regions indicated as GF1, GF2, and GF3 in Fig. 2. To exemplify the nature of this transition, we fix the parameter f at $f=0.1$ and vary A in the GF3 region. For $A=1.0$, the system exhibits quasiperiodic oscillation of period $1T$. The attractor undergoes a torus-doubling bifurcation as A is increased to $A=1.06$. On increasing the A value further, a second period doubling of the doubled torus does not take place. Instead, oscillations of the doubled torus in the amplitude direction start to appear at $A=2.165$ as shown in Fig. 5(a). As A is increased further to $A=2.167$, the oscillatory behavior of the torus gradually approaches a fractal nature. At such values, the nature of the attractor is strange [see Fig. 5(b)] even though the largest Lyapunov exponent in Fig. 6(a) remains negative. Such a phenomenon is essentially a gradual fractalization of the doubled torus as was shown by Nishikawa and Kaneko in their route to chaos via a SNA [9]. In this route, there is no collision involved among the orbits and therefore the Lyapunov exponent increases only slowly, as shown in Fig. 6(a), and there are no significant changes in its variance [see Fig. 6(b)]. Further, the phase sensitivity function Γ_N grows unboundedly with the power-law relation $\Gamma_N=N^{\mu}$, $\mu=0.83$, in the SNA region, while it is bounded in the torus region [see Fig. 6(c)]. At even higher values of A, $A=2.17$, the system exhibits chaotic oscillations ($C2$). The quantity Γ_N grows exponentially with N for the chaotic attractors.

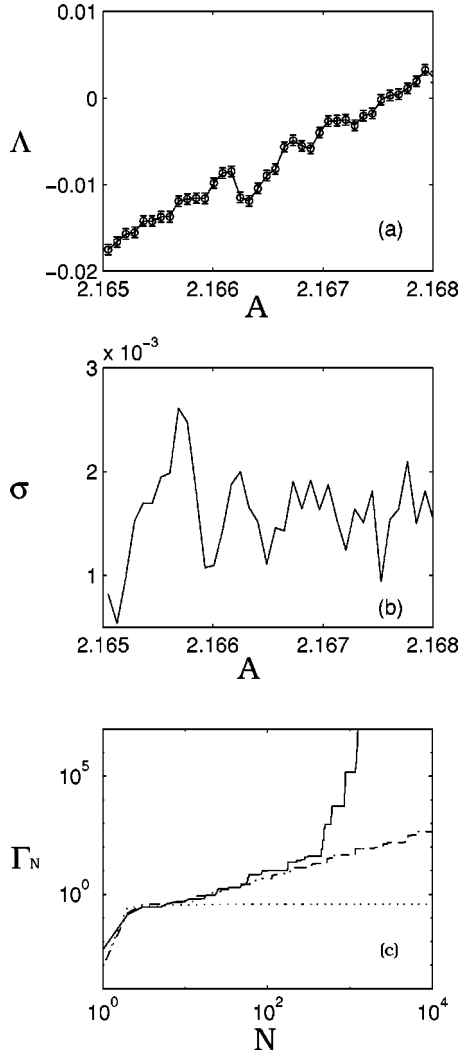

FIG. 6. Transition from doubled torus to SNA through gradual fractalization mechanism in the region GF3: (a) the behavior of the Lyapunov exponent (Λ); (b) the variance (σ); (c) plot of phase sensitivity function Γ_N vs N (dotted line corresponds to torus for $A=1.85$, dashed line belongs to SNA for $A=2.167$, and solid line represents chaos for $A=2.17$).

C. Type-III intermittent route

The third of the routes that is predominant in this system within the torus-doubled region is an intermittent route in which the torus-doubling bifurcation is tamed due to subharmonic bifurcations leading to the creation of a SNA. Such a phenomenon has been identified within the range of f values $0.33<f<0.41$ and on increasing the value of A, $1.81<A<2.18$, for a fixed f. To illustrate this transition, let us fix the parameter f at $f=0.35$ and vary A. For $A=1.0$, the attractor is a quasiperiodic attractor. As A is increased to $A=1.28$, the attractor undergoes a torus-doubling bifurcation. On increasing the value of A further, $A=2.13$, the attractor starts to wrinkle. On further increase of A to $A=2.135$, the attractor becomes extremely wrinkled and has several sharp bends, as shown in Fig. 7(a). It has been observed in lower dimensional chaotic systems [35,36] that when the system undergoes subcritical period-doubling bifurcation the dynamical

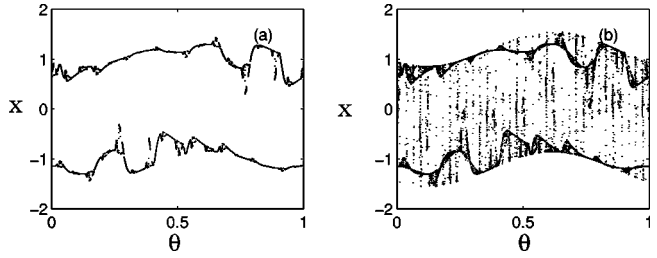

FIG. 7. Projection of the attractors of Eqs. (3) for $f=0.35$ in the (x,θ) plane indicating the transition from quasiperiodic attractor to chaotic attractor via a SNA through the type-III intermittent mechanism: (a) wrinkled attractor (period $2T$) for $A=2.135$; (b) SNA at $A=2.14$.

behavior exhibits type-III intermittent motion. In a similar manner, one finds that the wrinkled attractor undergoes a quasiperiodic analog of the subcritical period-doubling bifurcation on increasing the value of A further to $A=2.14$. The corresponding intermittent motion is shown in Fig. 7(b). The emergence of such intermittent dynamical behavior has been found in different continuous systems by the present authors and their collaborators through the intermittent route to chaos via SNA [17], where it was shown that during the transition from torus-doubled attractor to SNA growth of a subharmonic amplitude begins together with a decrease in the size of the fundamental amplitude. At the critical parameter value, the intermittent attractor loses its smoothness and becomes strange. The attractor shown in Fig. 7(b) is nothing but a strange nonchaotic one as the Lyapunov exponent turns out to be negative [Fig. 8(a)]. On examining the Lyapunov exponent at this transition, it is observed in Fig. 8(a) that the Lyapunov exponent shows an abrupt change with a power-law dependence on the parameter on the SNA side of the transition and the variance shows a remarkable and abrupt increase at the transition point as shown in Fig. 8(b). Further, the phase sensitivity function Γ_N is bounded for the torus region while it is unboundedly changing with a power-law variation with N for the SNA region [Fig. 8(c)] with $\mu=0.85$. On increasing the value of A further to $A=2.153$, we find the emergence of a chaotic attractor ($C2$) where the quantity Γ_N grows exponentially with N [Fig. 8(c)].

In the HH case, the points on the SNA are distributed over the entire region enclosed by the wrinkled bounding torus, while in the GF case the points on the SNA are distributed mainly on the boundary of the torus. Interestingly, in the present case shown in Fig. 7(b), most of the points of the SNA remain within the wrinkled torus with sporadic large deviations. The dynamics at this transition obviously involves a kind of intermittency. Such an intermittency transition could be characterized by scaling behavior. The laminar phase in this case is the torus while the burst phase is the nonchaotic attractor. In order to calculate the associated scaling constant, we coevolve the trajectories for two different values of A, namely, A_c and another value near to A_c, while keeping identical initial conditions (x_i,θ_i) as well as the same parameter value f. As the angular coordinate θ_i remains identical, the difference in x_i allows one to compute the av-

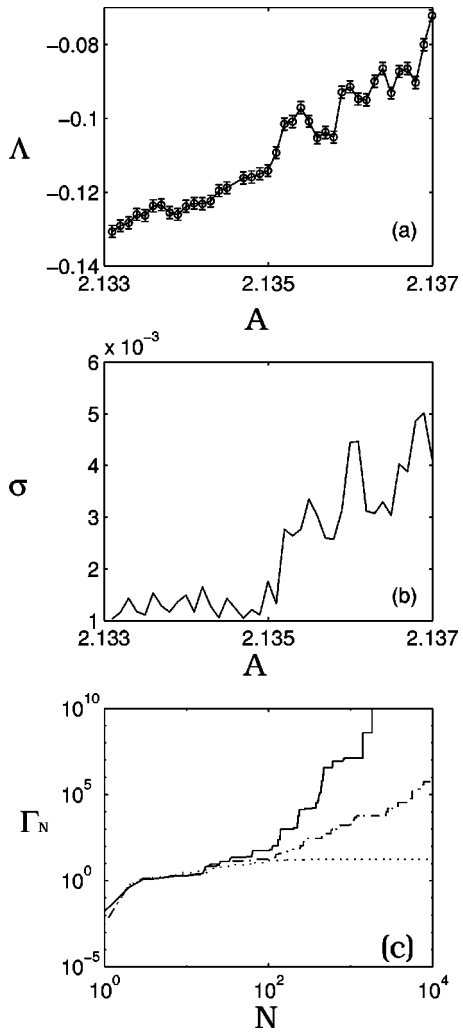

FIG. 8. Transition from doubled torus to SNA through type-III intermittent mechanism in the region $S3$: (a) the behavior of the Lyapunov exponent (Λ); (b) the variance (σ); (c) plot of phase sensitivity function Γ_N vs N (dotted line corresponds to torus for $A=1.83$, dashed line belongs to SNA for $A=2.14$, and solid line represents chaos for $A=2.15$).

erage laminar length between the bursts, and it fits the scaling form

$$\langle l\rangle=(A_c-A)^{-\alpha}. \tag{4}$$

The numerical value obtained for the attractor shown in Fig. 7(b) is $\alpha\sim1.1$ [see Fig. 9(a)]. To confirm further that the SNA attractor [Fig. 7(b)] is associated with intermittent dynamics, we plot the frequency of laminar periods of duration τ, namely, $N(\tau)$ in Fig. 9(b). It obeys the scaling [37] law

$$N(\tau)\sim\left\{\frac{\exp(-4\epsilon\tau)}{[1-\exp(-4\epsilon\tau)]}\right\}^{0.5}. \tag{5}$$

We find that $\epsilon=0.007\pm0.0002$ gives the best fit for the present data. These characteristic studies suggest that the intermittency is of type III as discussed by Pomeau and Manneville in low dimensional systems [36,37].

D. Crisis-induced intermittency

In the preceding subsections, we have seen that the period-doubling bifurcation of a torus has been truncated by its destruction, leading to the emergence of a SNA in certain regions of the (A-f) parameter space. Further, we observe that in the present system in some cross sections of the (A-f) parameter space the period-doubling phenomenon still persists in the destroyed torus even though the actual doubling phenomenon has been truncated. But in the present case it is observed that the doubling of the destroyed torus involves a kind of sudden widening of the attractor similar to the crisis phenomenon that occurs in chaotic systems. Such a phenomenon has been observed in the present model in a range of f values, $0.13<f<0.24$, and for a narrow range of A values, $2.12<A<2.14$. It is denoted as IC in Fig. 2. For example, let us choose $f=0.2$ and vary the value of A. For $A=0.8$, the attractor is a quasiperiodic one. As A is increased to $A=1.18$, the system undergoes torus-doubling bifurcation. On increasing the value of A further to $A=2.138$, the attractor begins to wrinkle as shown in Fig. 10(a). On increasing the value of A further, say, to $A=2.1387$ the wrinkled attractor undergoes torus-doubling bifurcation and the corresponding orbit is shown in Fig. 10(b). It is also seen from Figs. 10(b) and 10(c) that when A is slightly larger than $A_{IC}=2.1387$ the orbit on the attractor spends long stretches of time in the region to which the attractor was confined before the crisis. At the end of these long stretches the orbit bursts out of the old region and bounces around in the new region made available to it by the crisis. It then returns to the old region for another stretch of time, followed by a burst, and so on. This kind of widening of the attractor usually occurs in chaotic systems at a crisis [33]. However, in the present case, we

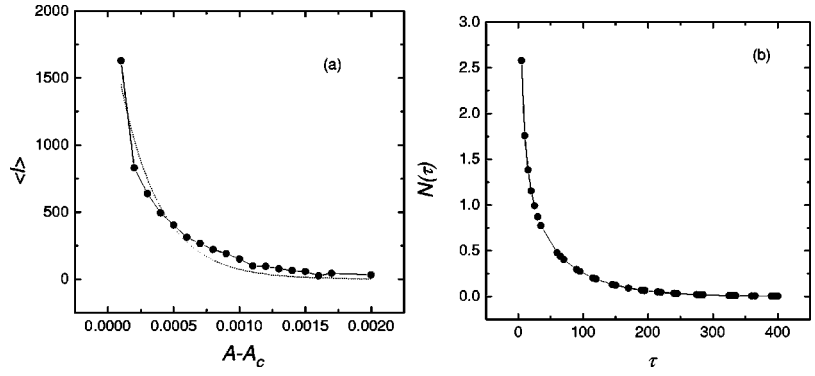

FIG. 9. (a) Average laminar length ($\langle l\rangle$) vs ($A-A_c$) at $f=0.35$; (b) number of laminar periods $N(\tau)$ of duration τ in the case of transition through type-III intermittency.

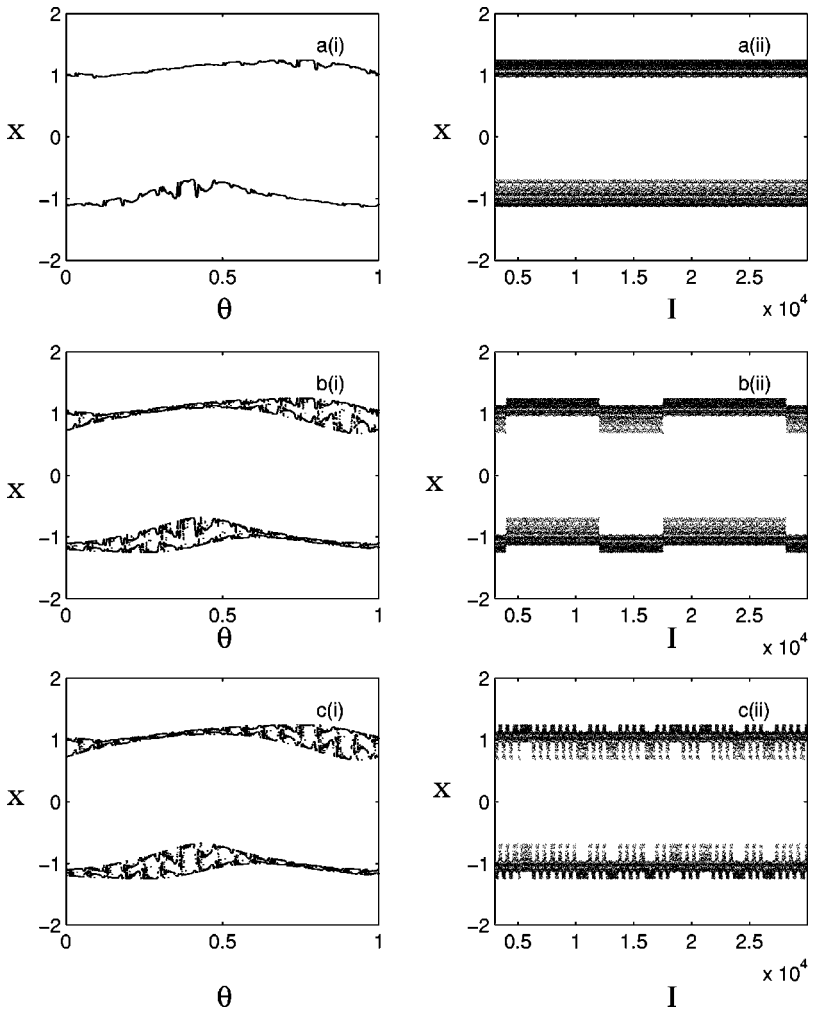

FIG. 10. Projection of the attractors of Eqs. (3) for $f=0.2$ (i) in the (x,θ) plane; (ii) in the (x,i) plane, indicating the transition from quasiperiodic attractor to chaotic attractor via a SNA through the crisis-induced intermittent mechanism: (a) wrinkled attractor (period $2T$) for $A=2.138$; (b) SNA at $A=2.1387$; (c) SNA at $A=2.1388$.

have shown such a possibility in a quasiperiodically forced system which also truncates the growth of the torus-doubled cascade, creating SNAs. The variation of the Lyapunov exponent at such a transition does not follow a uniform pattern, in contrast to the case of low dimensional chaotic systems exhibiting the crisis phenomenon [see Figs. 11(a) and 11(b)]. In addition, the phase sensitivity function Γ_N grows with N with a kind power-law relation for the SNA while it is bounded for the torus regions [see Fig. 11(c)]. On further increase of the value of A to $A=2.143$, the system exhibits chaotic oscillations ($C2$) and the quantity Γ_N grows exponentially with N.

V. DYNAMICS OUTSIDE THE TORUS BUBBLE

Two additional interesting transitions take place outside the torus bubble region, namely (1) gradual fractalization of the torus and (2) the type-I intermittent route, both leading to creation of a SNA. The details are as follows.

A. Fractalization route

The first mechanism is the gradual fractalization route, which is the same as studied in Sec. IV B; the only difference now is that here a transition from a one-frequency torus ($1T$) to chaos via the SNA is realized through the gradual fractalization process instead of the transition from the $2T$ torus discussed above. Such a phenomenon is identified in the lower side of the $C1$ region (GF4) in Fig. 2. Specifically, within the region $0.58<f<0.8$, on increasing the value of A to the region $1.211<A<1.569$ for a fixed f, the SNA is created through the gradual fractalization route. First, a transition from the one-frequency torus to a wrinkled attractor takes place on increasing A, $A=1.25$ for $f=0.7$, as shown in Fig. 12(a). The wrinkled attractor loses its continuity considerably as A is increased further and then finally becomes fractal at $A=1.265$ [see Fig. 12(b)]. It is very obvious from these transitions that the torus gradually loses its smoothness and ultimately approaches fractal behavior via a SNA before the onset of chaos as the parameter A increases to $A=1.3$. In addition, it is observed that there is no apparent interaction among the orbits. This property has been confirmed through the calculation of the maximal Lyapunov exponent, its variance, and the phase sensitivity as in the period-doubled regions.

B. Type-I intermittent route

A different type of intermittent route, namely, type I [21], via the SNA is also observed in the upper region of $C1$ in Fig. 2. Within the range of values $0.58<f<0.8$, on increas-

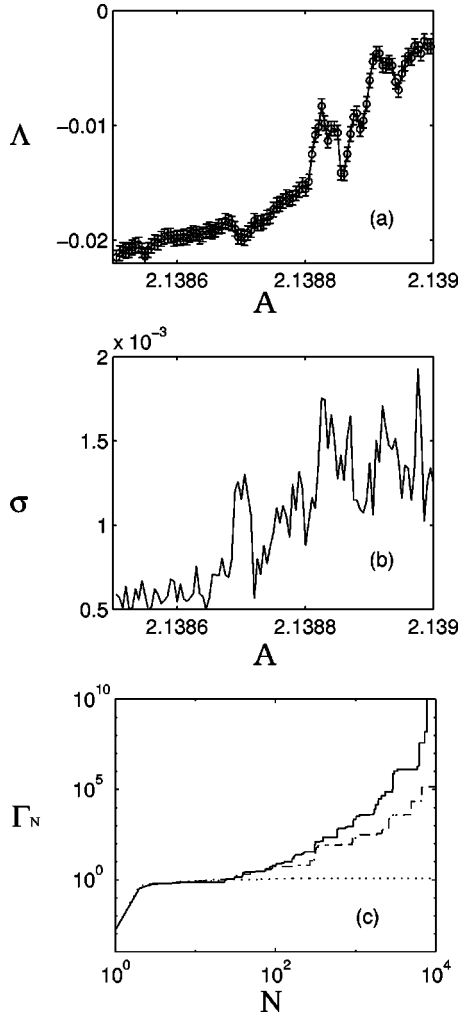

FIG. 11. Transition from doubled torus to SNA through crisis-induced intermittency mechanism in the region IC: (a) the behavior of the Lyapunov exponent (Λ); (b) the variance (σ); (c) plot of phase sensitivity function Γ_N vs N (dotted line corresponds to torus for $A=1.83$, dashed line belongs to SNA for $A=2.1388$, and solid line represents chaos for $A=2.139$).

ing the value of A in the range $1.5<A<2.0$, a transition from the chaotic attractor ($C1$) to a SNA takes place first and then the SNA is eventually replaced by a one-frequency quasiperiodic orbit through a quasiperiodic analog of saddle-node

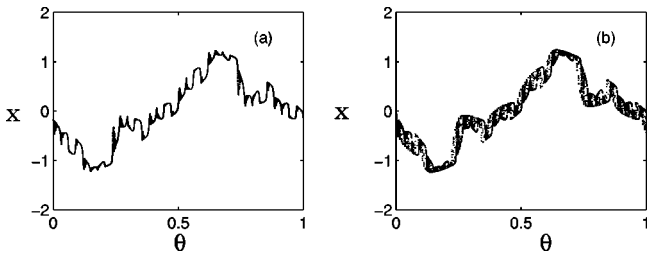

FIG. 12. Projection of the attractors of Eqs. (3) for $f=0.7$ in the (x,θ) plane indicating the transition from a one-frequency quasiperiodic attractor to a chaotic attractor via a SNA through the gradual fractalization mechanism: (a) wrinkled attractor (period $1T$) for $A=1.25$; (b) SNA at $A=1.265$.

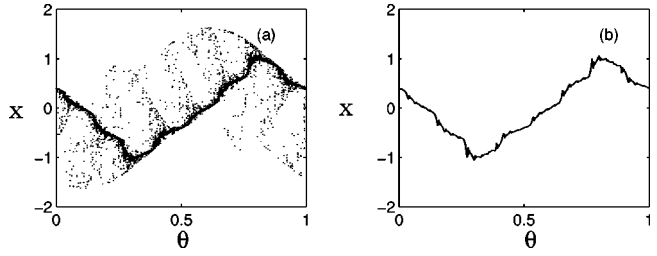

FIG. 13. Projection of the attractors of Eqs. (3) for $f=0.7$ in the (x,θ) plane indicating the transition from a one-frequency quasiperiodic attractor to a chaotic attractor via a SNA through the type-I intermittency mechanism: (a) intermittent SNA for $A=1.801\,685$; (b) torus at $A=1.8017$.

bifurcation. At this transition, the dynamics is found to be again intermittent but of a different type.

To understand more about this phenomenon, let us consider the specific parameter value $f=0.7$ and vary A. For $A=1.801\,65$, the attractor is a chaotic one ($C1$). As A is increased to $A=1.801\,685$, the chaotic attractor transits to a SNA as shown in Fig. 13(a). On increasing the value of A further, an intermittent transition from the SNA to a torus as shown in Fig. 13(b) occurs at $A=1.8017$. At this transition, abrupt changes in the Lyapunov exponent as well as its variance show the characteristic signature of the intermittent route [indicated in Figs. 14(a) and 14(b)] to SNA as in the type-III case. In addition, again the quantity Γ_N grows with N with a power-law relation for the SNA while it is bounded for the torus regions [see Fig. 14(c)]. However, in the chaotic region, the quantity Γ_N grows exponentially with N.

Further, the plot of laminar length $\langle l\rangle$ as a function of the derived bifurcation parameter $\epsilon=A-A_c$, where A_c is the critical parameter for the occurrence of the intermittent transition, for this attractor reveals a power-law relationship of the form

$$\langle l\rangle=\epsilon^{-\beta}, \tag{6}$$

with an estimated value of $\beta\sim0.53$ [Fig. 15(a)]. Also, the plot of the number of laminar periods $N(\tau)$ vs the period length τ [shown in Fig. 15(b)] indicates that after an initial steep decay there is an increase to a large value of $N(\tau)$. It also obeys the relation

$$N(\tau)\sim\frac{\epsilon}{2c}\left\{\tau+\tan\left[\arctan\left(\frac{c}{\sqrt{\epsilon/u}}\right)-\tau\sqrt{\epsilon u}\right]-\arctan\left(\frac{c}{\sqrt{\epsilon/u}}\right)\tau-\tau^2\sqrt{\frac{\epsilon}{u}}\right\}, \tag{7}$$

where c is the maximum value of $x(t)$, $u=0.9$, and $\epsilon=0.0005\pm0.000\,03$. The above analysis confirms that such an attractor is associated with the standard intermittent dynamics of type I described in Refs. [36,37].

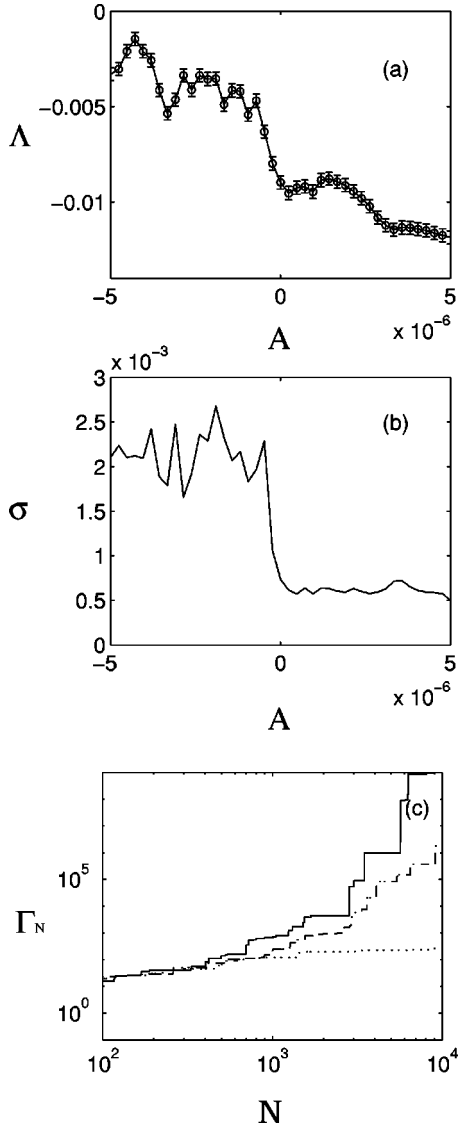

FIG. 14. Transition from intermittent SNA to a torus through the type-I intermittent mechanism in the region $S1$: (a) the behavior of the Lyapunov exponent (Λ); (b) the variance (σ); (c) plot of phase sensitivity function Γ_N vs N (dotted line corresponds to torus for $A=1.8017$, dashed line belongs to SNA for $A=1.801\,685$, and solid line represents chaos for $A=1.8015$).

VI. TRANSITION BETWEEN DIFFERENT SNAs

In the preceding sections, we have enumerated the several ways by which SNAs are created from torus attractors. One might observe from the (A-f) phase diagram, Fig. 2, that there are several regions where transitions from one type of SNA to another type occur along the borders separating quasiperiodic and chaotic attractors. In particular, transitions occur between GF3 and IC, IC and GF2, GF2 and $S3$, $S3$ and GF1, GF1 and HH, and $S1$ and GF4. On closer scrutiny, we find that there exists a very narrow range of parameters between different regions of SNAs where chaotic motion occurs. That is, the SNA of one region transits to chaos before exhibiting a different type of SNA in the next region. However, we refrain from giving finer details as they do not seem to be of significance.

VII. SIGNATURES OF FINITE-TIME LYAPUNOV EXPONENTS AT THE TRANSITION TO DIFFERENT SNAs

Recently, it was noted by Prasad, Mehra, and Ramaswamy [21] that a typical trajectory on a SNA actually possesses positive Lyapunov exponents in finite time intervals, although the asymptotic exponent is negative. As a consequence, one observes the different characteristics of SNAs created through different mechanisms by a study of the differences in the distribution of finite-time exponents $P(N,\lambda)$ [21]. For each of the cases, the distribution can be obtained by taking a long trajectory and dividing it into segments of length N, from which the local Lyapunov exponent can be calculated. In the limit of large N, this distribution will collapse to a δ function $P(N,\lambda)\rightarrow\delta(\Delta-\lambda)$. The deviations from, and the approach to, the limit can be very different for SNAs created through different mechanisms. Figures 16 illustrate the distributions for $P(50,\delta)$ across the five different transitions discussed in the present study. A common feature of these cases is that $P(N,\lambda)$ is strongly peaked about the Lyapunov exponent when the attractor is a torus, but on the SNA the distribution picks up a tail which extends into the local Lyapunov exponent $\lambda>0$ region. This tail is directly correlated with enhanced fluctuation in the Lyapunov exponent on SNAs. On the fractalized SNA and on doubling of the SNA, the distribution shifts continuously to larger Lyapunov exponents, but the shape remains the same for torus regions as well as SNA regions, while on the HH and intermittent SNA routes, the actual shapes of the distribution on the torus and the SNA are very different. One remarkable feature of intermittent SNAs is that the positive tail in the distribution decays very slowly.

To quantify further the distribution of finite-time Lyapunov exponents, let us consider, for example, the fraction of exponents lying above $\lambda=0$, $F_+(N)$, vs N for the different SNAs. It has been found that, except for the intermittent SNA (for both types III and I), for which $F_+(N)\sim N^{-\beta}$, this quantity decays exponentially, $F_+(N)\sim\exp(-\gamma N)$ for all other transitions, with the exponents β and γ dependent strongly on the parameters of the system. For the specific SNAs corresponding to the parameters reported in the previous section these quantities take the following values. For type-III and type-I intermittency, the β values are 0.38 and 0.71. However, for HH, GF, and IC, the β and α values are 0.27 and 0.32, 0.31 and 0.17, and 0.24 and 0.34, respectively.

VIII. CONCLUSION

In this paper we have described the creation of SNAs through various routes and mechanisms in a protypical example, namely, the quasiperiodically driven cubic map. These are summarized in Table I. Torus-doubling bifurcations are not mandatory for the creation of SNAs. However, they are merely a convenient agent in setting the stage for the appearance of SNAs. There are at least four different mechanisms, namely, Heagy-Hammel, gradual fractalization, and type-III and crisis-induced intermittency, through which the truncation of torus doubling and the creation of SNAs occur. The truncation of torus-doubling and the genesis of

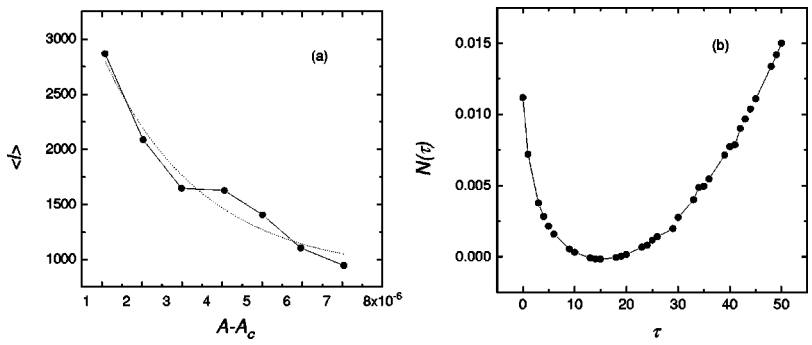

FIG. 15. (a) Average laminar length ($\langle l \rangle$) vs ($A-A_c$) at $f=0.7$; (b) number of laminar periods $N(\tau)$ of duration τ in the case of transition through type-I intermittency.

SNAs through crisis-induced intermittency is entirely different from the interior crisis mechanism for the appearance of SNAs found by Witt *et al.* [38]. We have further observed at least two different ways, namely, type-I intermittency and gradual fractalization, through which SNAs are formed when a transition from a one-frequency torus to chaos takes place. All these phenomena have been identified in a two parameter (A-f) phase diagram. To distinguish among the different mechanisms through which SNAs are created, we have examined the manner in which the maximal Lyapunov exponent and its variance change as a function of the parameters. In addition, we have also examined the distribution of local Lyapunov exponents and found that on different SNAs they have different characteristics. The analysis confirms that in the intermittent SNAs the signature of the transition is a discontinuous change in both the maximal Lyapunov exponent and the variance. The chaotic component on the intermittent SNA is long lived. As a consequence, a slow positive tail in $P(N,\lambda)$ and a resulting power-law decay for $F_+(N)$ can be identified. For the other SNAs, a resulting exponential decay for $F_+(N)$ has been identified.

ACKNOWLEDGMENTS

This work was supported by the Department of Science and Technology, Government of India. A.V. wishes to acknowledge the Council of Scientific and Industrial Research, Government of India, for financial support.

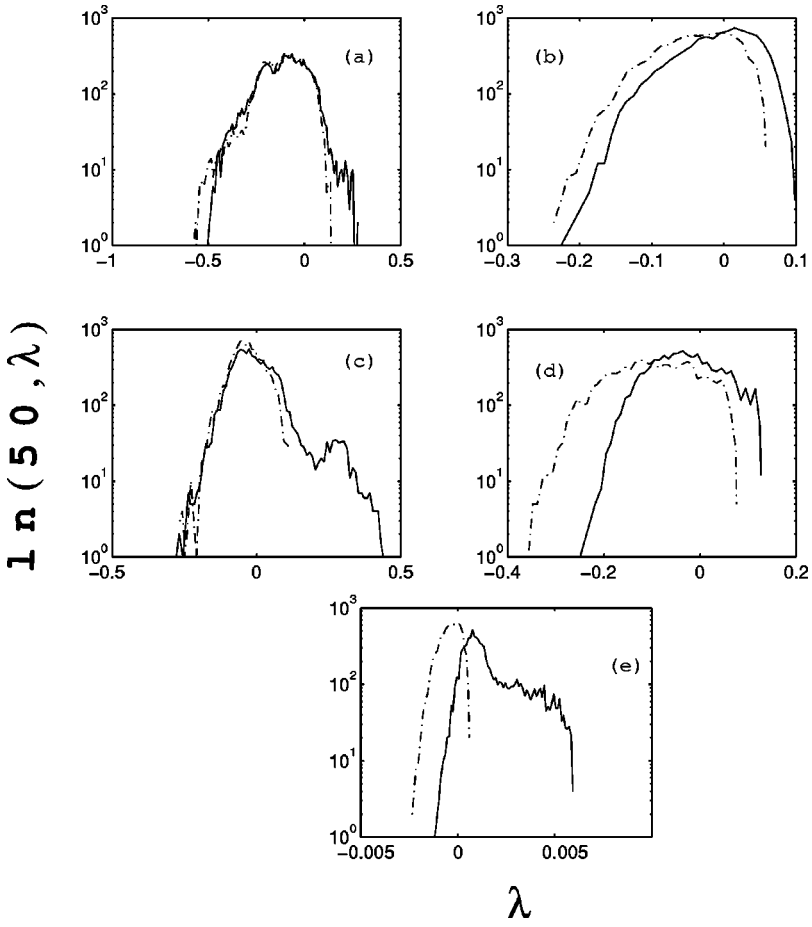

FIG. 16. Distribution of finite-time Lyapunov exponents on SNAs created through (a) the Heagy-Hammel mechanism, (b) gradual fractalization, (c) type-III intermittency, (d) crisis-induced intermittency, and (e) type-I intermittency. Solid and dashed lines correspond to SNA and torus distributions.

TABLE I. Routes and mechanisms of the onset of various SNAs in the quasiperiodically forced cubic map.

Type of route	Mechanism	Characteristic properties: Lyapunov exponent λ	Variance σ	Fraction of positive valued finite-time Lyapunov exponents $[F_+(N,\lambda)]$	Scaling law $\langle l \rangle \sim (A_c - A)^{\alpha}$	Figures
		A. Interruption of torus-doubling				
1. Heagy-Hammel [8]	Collision between a period-doubled torus and its unstable parent	Irregular in SNA region and smooth in torus	Small in torus and large in SNA	Decays exponentially		3 and 4
2. Gradual fractalization [9]	Torus gets increasingly wrinkled and transforms into a SNA without any interaction with a nearby unstable periodic orbit	Increases slowly during the transition from torus to SNA	No significant changes	Decays exponentially		5 and 6
3. Type-III intermittency [19]	During the transition from torus-doubled attractor to SNA, a growth of subharmonic amplitude begins, together with a decrease in the size of the fundamental amplitude	Abrupt change during the transition from torus to SNA	Abrupt increase at the transition point	Power-law variation	$\alpha \sim 1.1$ [see also Eq. (5)]	7, 8, and 9
4. Crisis-induced intermittency	Doubling of destroyed torus involves a kind of sudden widening of the attractor	Does not follow uniform pattern	Irregular variation in SNA region	Decays exponentially		10 and 11
		B. Transition from one-frequency torus				
1. Gradual fractalization [9]	Torus gets increasingly wrinkled and transforms into a SNA	Increases slowly during the transition from torus to SNA	No significant change	Decays exponentially		12
2. Type-I intermittency [21]	Torus is eventually replaced by SNA through an analog of the saddle-node bifurcation	Abrupt change during the transition from torus to SNA	Abrupt increase at the transition point	Power-law variation	$\alpha \sim 0.55$ [see also Eq. (7)]	13, 14, and 15,

APPENDIX: CHARACTERIZATIONS OF THE SNA

1. Phase sensitivity exponent

In order to distinguish between the smooth and the fractal torus (SNA and chaos), we examine the attractor with reference to the phase θ of the external force. Even though no exponential divergence of orbits exists for either the smooth or the fractal torus (SNA), they are different from each other in terms of the phase sensitivity. Pikovsky and Feudal [23,24] have shown how two points on the SNA that have close θ values can be separated from each other by introducing the phase sensitivity exponent. To appreciate this, we note that the absolute value of the first derivative of the orbit $|\partial x_n/\partial \theta_n|$ fluctuates with time and sometimes has large bursts. To see this, one can proceed as follows. An arbitrarily large burst can appear when the system is iterated for infinite time steps. By differentiating Eq. (3), one obtains

$$\frac{\partial x_{n+1}}{\partial \theta} = -2\pi Q \sin(2\pi\theta) - (A - 3x_n^2)\frac{\partial x_n}{\partial \theta}. \tag{A1}$$

So, starting from a suitable initial derivative $|\partial x_0/\partial\theta|$, one can obtain derivatives at all points of the trajectory,

$$\frac{\partial x_N}{\partial \theta} = S_N = \sum_{k=1}^{N} \left\{ -2\pi Q \sin(2\pi\theta_{k-1}) \times \left[\prod_{i=0}^{N-k-1} -(A - 3x_{k+i}^2) \right] \right\} + \prod_{i=0}^{N-1} \left(-(A - 3x_i^2)\frac{\partial x_0}{\partial \theta} \right), \tag{A2}$$

with the condition that for $k = N$

$$\prod_{i=0}^{N-k-1} [-(A - 3x_{k+i}^2)] = 1.$$

Naturally, in the case of a smooth attractor, if one iterates Eqs. (A1) and (A2) starting from aribitrary values of x and $\partial x/\partial\theta$ and for large N, they converge to the attractor and its derivative, respectively. Thus, partial sums S_N computed from (A2) are bounded by the maximum derivative $\partial x/\partial\theta$ along the attractor. But in the case of a fractal attractor the attractor is nonsmooth and the derivative $\partial x/\partial\theta$ does not exist, so the consideration above is no longer valid. This can be illustrated by calculating the partial sums S_N as given by Eq. (A2). It has been found [23,24] that the behavior of the sum can be very intermittent. The key observation is that these sums are quite large and essentially unbounded. Hence, we plot the maximum of $|S_N|$,

$$\gamma_N(x,\theta)=\max|S_N|. \tag{A3}$$

The value of γ_N grows with N, which means that arbitrarily large values of $|S_N|$ appear. From this it follows immediately that the attractor cannot have a finite derivative with respect to the external phase if the attractor is nonsmooth. Consequently, the assumption of a finite derivative is inconsistent with the relation (A2), where the second term on the right-hand side (RHS) is exponentially small and the first term on the RHS can be arbitrarily large. Thus, by calculating the partial sums (A2), we can distinguish between strange (sums are unbounded) and nonstrange (sums are bounded) attractors.

The growth rate of the partial sums with time represents the degree of strangeness of the attractor, and can be used as a quantitative characteristic of SNAs. For this purpose, we require a quantity that is independent of a particular trajectory while it represents the average properties of the attractor. The appropriate quantity seems [23,24] to be the minimum value of $\gamma_N(x,\theta)$ with respect to randomly chosen initial points (x,θ):

$$\Gamma_N=\min\gamma_N(x,\theta). \tag{A4}$$

It allows a more reliable inference about whether the attractor is nonsmooth. One can also infer from Eq. (A4) that Γ_N grows infinitely for a SNA with some relation such as $\Gamma_N=N^{\mu}$, where μ is a positive quantity that characterizes the SNA; we call it the phase sensitivity exponent. However, in the case of a chaotic attractor, it grows exponentially with N.

2. Variation of finite-time Lyapunov exponents

Since the finite-time or local Lyapunov exponents $(\lambda_i, i=1,2,\ldots,M)$ depend on the initial conditions, it will be relevant to consider the variance of the average Lyapunov exponent Λ about the λ_i's, $i=1,2,\ldots,M$. It is defined [17,21,33,39] as

$$\sigma=\frac{1}{M}\sum_{i=1}^{M}[\Lambda-\lambda_i(N)]^2. \tag{A5}$$

In all our numerical calculations, we take $N=50$ and $M\cong 10^5$.

The variation of the local Lyapunov exponents in a fixed time interval t can also be discussed by examining the probability distributions $P(t,\lambda)$ for the exponents. In fact, $P(t,\lambda)$ corresponds to counting the normalized number of times any one of the λ appears for fixed time t. That is, the distribution of local Lyapunov exponents, which is a stationary quantity, is defined as [33]

$$P(t,\lambda)d\lambda\equiv\text{probability that } \lambda(t) \text{ takes a value between } \lambda \text{ and } \lambda+d\lambda. \tag{A6}$$

This is particularly useful in describing the structure and dynamics of nonuniform attractors. In the asymptotic limit $t\to\infty$, this distribution will collapse to a δ function,

$$P(t,\lambda)\to\delta(\Lambda-\lambda).$$

The deviations from this limit for finite times, and the asymptotics, namely, the approach to the limit, can be very revealing of the underlying dynamics [21].

One can also calculate the arithmetic mean of all the distributions and obtain the variance of the Lyapunov exponent Λ as

$$\sigma=\int_{-\infty}^{\infty}(\Lambda-\lambda)^2P(t,\lambda)d\lambda. \tag{A7}$$

Dividing the total length of the orbit into M bins as before and defining the local Lyapunov exponents as λ_i, replacing $P(t,\lambda_i)$ by $\delta(\Lambda-\lambda_i)/M$, the above equation of variance goes over to the form given by Eq. (A5).

3. Power spectrum analysis

To quantify the changes in the power spectrum (obtained using the fast Fourier transform technique), one can compute the so called spectral distribution function $N(\sigma)$, defined to be the number of peaks in the Fourier amplitude spectrum larger than some value, say σ. Scaling relations have been predicted for $N(\sigma)$ in the case of two- and three-frequency quasiperiodic attractors and strange nonchaotic attractors. These scaling relations are $N(\sigma)\sim\ln(1/\sigma)$, $N(\sigma)\sim\ln^2\sigma$, and $N(\sigma)\sim\sigma^{-\beta}$, respectively, corresponding to the two- and three-frequency quasiperiodic and strange nonchaotic attractors. In the work of Ding *et al.* [13], the power-law exponent was found empirically to lie within the range $1<\beta<2$ for the strange nonchaotic attractor.

4. Dimensions

To quantify geometric properties of attractors, several methods have been used to compute the dimension of the attractors. From them, we have used the correlation dimension (introduced by Grassberger and Procaccia [40]) in our present study, which may be computed from the correlation function $C(R)$ defined as

$$C(R)=\lim_{N\to\infty}\left[\frac{1}{N^2}\sum_{i,j=1}^{N}H(R-|x_i-x_j|)\right],$$

where x_i and x_j are points on the attractor, $H(y)$ is the Heaviside function (1 if $y \geqslant 0$ and 0 if $y<0$), and N is the number of points randomly chosen from the entire data set. The Heaviside function simply counts the number of points within the radius R of the point denoted by x_i and $C(R)$ gives the average fraction of points. Now the correlation dimension is defined by the variation of $C(R)$ with R:

$$C(R) \sim R^d \quad \text{as} \quad R \to 0.$$

Therefore the correlation dimension (d) is the slope of a graph of $\log_{10} C(R)$ versus $\log_{10} R$. Once one obtains the dimensions of the attractors, it is easy to quantify the strange property of the attractors. In all our studies, we have verified that the SNAs have noninteger correlation dimensions.

[1] K. Kaneko, *Collapse of Tori and Genesis of Chaos in Dissipative Systems* (World Scientific, Singapore, 1986).
[2] V. Franceschini, Physica D **6**, 285 (1983).
[3] A. Arenéodo, P.H. Coullet, and E.A. Speigel, Phys. Lett. **94A**, 1 (1983).
[4] J.M. Flesselles, V. Croquette, and S. Jucquois, Phys. Rev. Lett. **72**, 2871 (1994).
[5] K.E. Mckell, D. Broomhead, R. Jones, and D.T.J. Hurle, Europhys. Lett. **12**, 513 (1990).
[6] M.R. Basset and J.L. Hudson, Physica D **35**, 289 (1989).
[7] J.E. Kim, H.K. Park, and H.T Moon, Phys. Rev. E **55**, 3948 (1997).
[8] J.F. Heagy and S.M. Hammel, Physica D **70**, 140 (1994).
[9] K. Kaneko, Prog. Theor. Phys. **71**, 140 (1994); T. Nishikawa and K. Kaneko, Phys. Rev. E **54**, 6114 (1996).
[10] S. Kuznetsov, U. Feudal, and A. Pikovsky, Phys. Rev. E **57**, 1585 (1998).
[11] A. Venkatesan and M. Lakshmanan, Phys. Rev. E **55**, 4140 (1997); **58**, 3008 (1998).
[12] C. Grebogi, E. Ott, S. Pelikan, and J.A. Yorke, Physica D **13**, 261 (1984); C. Grebogi, E. Ott, F.J. Romeiras, and J.A. Yorke, Phys. Rev. A **36**, 5365 (1987).
[13] M. Ding, C. Grebogi, and E. Ott, Phys. Rev. A **39**, 2593 (1989); F.J. Romeiras and E. Ott, *ibid.* **35**, 4404 (1987).
[14] F.J. Romeiras, A. Bonderson, E. Ott, T.M. Andonsen, Jr., and C. Grebogi, Physica D **26**, 277 (1987); A. Bonderson, E. Ott, and T.M. Andonsen, Jr., Phys. Rev. Lett. **55**, 2103 (1985).
[15] M. Ding and J.A. Scott Relso, Int. J. Bifurcation Chaos Appl. Sci. Eng. **4**, 553 (1994).
[16] J.F. Heagy and W.L. Ditto, J. Nonlinear Sci. **1**, 423 (1991).
[17] A. Venkatesan, M. Lakshmanan, A. Prasad, and R. Ramaswamy, Phys. Rev. E **61**, 3641 (2000).
[18] T. Yalcinkaya and Y.C. Lai, Phys. Rev. Lett. **77**, 5040 (1996); Phys. Rev. E **56**, 1623 (1997).
[19] A. Venkatesan, K. Murali, and M. Lakshmanan, Phys. Lett. A **259**, 246 (1999).
[20] Z. Liu and Z. Zhua, Int. J. Bifurcation Chaos Appl. Sci. Eng. **6**, 1383 (1996); Z. Zhua and Z. Liu, *ibid.* **7**, 227 (1997); T. Yang and K. Bilimgut, Phys. Lett. A **236**, 494 (1997).
[21] A. Prasad, V. Mehra, and R. Ramaswamy, Phys. Rev. Lett. **79**, 4127 (1997); Phys. Rev. E **57**, 1576 (1998).
[22] Y.C. Lai, Phys. Rev. E **53**, 57 (1996); Y.C. Lai, U. Feudel, and C. Grebogi, *ibid.* **54**, 6114 (1996).
[23] A.S. Pikovsky and U. Feudal, Chaos **5**, 253 (1995); U. Feudal, J. Kurths, and A.S. Pikovsky, Physica D **88**, 176 (1995).
[24] A.S. Pikovsky and U. Feudal, J. Phys. A **27**, 5209 (1994); S.P. Kuznetsov, A.S. Pikovsky, and U. Feudel, Phys. Rev. E **51**, R1629 (1995).
[25] T. Kapitaniak and J. Wojewoda, *Attractors of Quasiperiodically Forced Systems* (World Scientific, Singapore, 1993); T. Kapitaniak, Phys. Rev. E **47**, 1408 (1993); T. Kapitaniak and L.O. Chua, Int. J. Bifurcation Chaos Appl. Sci. Eng. **7**, 423 (1997).
[26] V.S. Anishchensko, T.K. Vadivasova, and O. Sosnovtseva, Phys. Rev. E **53**, 4451 (1996); O. Sosnovtseva, U. Feudel, J. Kurths, and A. Pikovsky, Phys. Lett. A **218**, 255 (1996).
[27] W.L. Ditto, M.L. Spano, H.T. Savage, S.N. Rauseo, J.F. Heagy, and E. Ott, Phys. Rev. Lett. **65**, 533 (1990).
[28] T. Zhou, F. Moss, and A. Bulsara, Phys. Rev. A **45**, 5394 (1992).
[29] W.X. Ding, H. Deutsch, A. Dingklage, and C. Wilke, Phys. Rev. E **55**, 3769 (1997).
[30] M. Lakshmanan and K. Murali, *Chaos in Nonlinear Oscillators: Synchronization and Controlling* (World Scientific, Singapore, 1996).
[31] J. Guckenheimer and P. Holmes, *Nonlinear Oscillations, Dynamical Systems, and Bifurcation of Vector Fields* (Springer-Verlag, New York, 1983).
[32] M. Bier and T. Bountis, Phys. Lett. **104A**, 239 (1983).
[33] E. Ott, *Chaos in Dynamical Systems* (Cambridge University Press, Cambridge, 1994).
[34] A. Jackson, *Perspectives of Nonlinear Dynamics* (Cambridge University Press, New York, 1991).
[35] H.E. Nusse and J. Yorke, Phys. Lett. A **127**, 328 (1988).
[36] Y. Pomeau and P. Manneville, Commun. Math. Phys. **74**, 189 (1980).
[37] H.G. Schuster, *Deterministic Chaos* (Physik-Verlag, Weinheim, 1984).
[38] A. Witt, U. Feudel, and A. Pikovsky, Physica D **109**, 180 (1997).
[39] G. Benettin, L. Galgani, and J.-M. Strelcyn, Phys. Rev. A **14**, 2338 (1976).
[40] P. Grassberger and I. Procaccia, Physica D **9**, 189 (1983).